Tolerance of the MIMOSIS-1 CMOS Monolithic Active Pixel Sensor to ionizing radiation

H. Darwish, J. Andary, B. Arnoldi-Meadows, O. Artz, J. Baudot, G. Bertolone, A. Besson, N. Bialas, R. Bugiel, G. Claus, et al.

Tolerance of the MIMOSIS-1 CMOS Monolithic Active Pixel Sensor to ionizing radiation

Jinst

Published by IOP Publishing for Sissa Medialab

Received: *September 30, 2022*
Revised: *March 14, 2023*
Accepted: *March 23, 2023*
Published: *June 12, 2023*

23rd International Workshop on Radiation Imaging Detectors
26–30 June 2022
Riva del Garda, Italy

Tolerance of the MIMOSIS-1 CMOS Monolithic Active Pixel Sensor to ionizing radiation

H. Darwish,[a,b,c,*] **J. Andary,**[a] **B. Arnoldi-Meadows,**[a] **O. Artz,**[a] **J. Baudot,**[b] **G. Bertolone,**[b] **A. Besson,**[b] **N. Bialas,**[a] **R. Bugiel,**[b] **G. Claus,**[b] **C. Colledani,**[b] **M. Deveaux,**[c] **A. Dorokhov,**[b] **G. Dozière,**[b] **Z. El Bitar,**[b] **I. Fröhlich,**[a,c] **M. Goffe,**[b] **F. Hebermehl,**[a] **A. Himmi,**[b] **C. Hu-Guo,**[b] **K. Jaaskelainen,**[b] **O. Keller,**[f] **M. Koziel,**[a] **F. Matejcek,**[a] **J. Michel,**[a] **F. Morel,**[b] **C. Müntz,**[a] **H. Pham,**[b] **C.J. Schmidt,**[c] **S. Schreiber,**[a] **M. Specht,**[b] **D. Spicker,**[a] **J. Stroth,**[a,c,d] **I. Valin,**[b] **R. Weirich,**[a] **Y. Zhao**[b] **and M. Winter**[e]

[a] *Goethe-Universität Frankfurt, Frankfurt am Main, Germany*
[b] *Université de Strasbourg, CNRS, IPHC UMR 7178, Strasbourg, France*
[c] *GSI Helmholtzzentrum für Schwerionenforschung GmbH, Darmstadt, Germany*
[d] *Helmholtz Forschungsakademie Hessen für FAIR, Frankfurt am Main, Germany*
[e] *IJCLab, UMR9012 — CNRS, Université Paris-Saclay, Orsay, France*
[f] *Facility for Antiproton and Ion Research in Europe GmbH, Darmstadt, Germany*

E-mail: h.darwish@gsi.de

Abstract: MIMOSIS is a CMOS Monolithic Active Pixel Sensor (CPS) developed to equip the Micro Vertex Detector (MVD) of the Compressed Baryonic Matter (CBM) experiment at FAIR/GSI. The sensor will combine a spatial resolution of -5 µm with a time resolution of 5 µs and provide a peak hit rate capability of ~80 MHz/cm^2. To fulfil its task, MIMOSIS will have to withstand ionising radiation doses of ~5 MRad and fluences of $\sim 7 \times 10^{13}$ n_{eq}/cm^2 per year of operation.

The paper summarises major requirements of the CBM-MVD and compares them to the detection performances of the first full scale prototype, called MIMOSIS-1, recently evaluated in the laboratory and with particle beams. The tolerance of the sensor to the expected ionising radiation load was evaluated; the paper describes the measurements performed and their outcome.

Keywords: Particle tracking detectors (Solid-state detectors); Pixelated detectors and associated VLSI electronics; Radiation-hard detectors; Si microstrip and pad detectors

*Corresponding author.

https://doi.org/10.1088/1748-0221/18/06/C06013

Contents

1 Introduction

The MIMOSIS CPS will equip the Micro Vertex Detector (MVD) [1] of the Compressed Baryonic Matter (CBM) experiment [2], which is being built at the FAIR facility in Darmstadt, Germany. The fixed target experiment will explore the QCD phase diagram in the region of high baryon densities and probe the related hot and dense baryonic matter with rare probes such as di-leptons, multi-strange and (open) charm particles. CBM will create this hot and dense matter by means of heavy ion (resp. p+A) collisions at various beam energies ranging up to 10 *A*GeV (resp. 28 GeV). The collision rate will amount 100 kHz (resp. 10 MHz with p+A collisions) if the MVD is used. It may be further increased to 10 MHz (Au+Au collisions), if this detector is removed.

The MVD will be operated in the target vacuum at 5–20 cm downstream of the experimental target and as close as 5.5 mm from the beam axis. The requirements on the MVD and MIMOSIS are motivated by the need to reconstruct the secondary decay vertex of open charm particles. To match this goal, the sensor should provide a spatial resolution of ~5 µm. Thinning it to ~50 µm (0.05% X_0) will allow to achieve an overall material budget of 0.3% X_0 for the first detector station.

The MVD will have to withstand integrated radiation doses of 5 MRad and 7×10^{13} n_{eq}/cm^2 per CBM year of operation. Most ionising radiation is caused by δ-electrons kicked out of the target by the primary beam. While being partially deflected by the field of the 1 Tm dipole magnet of CBM, the majority of the electrons penetrate the MVD stations within a few cm^2 wide hot-spot located nearby the beam axis. This hot-spot, as well as the fixed target geometry of CBM, create sizeable gradients of radiation doses over the sensor, which may reach one order of magnitude. Moreover, the sensors will be exposed to $\lesssim 1$ kHz/cm^2 nuclear fragments and beam halo ions and must resist to beam impacts as caused by beam steering mistakes. This issue is discussed in [3].

2023 JINST 18 C06013

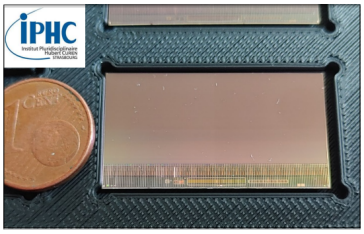

Figure 1. Photograph of the MIMOSIS-1 sensor.

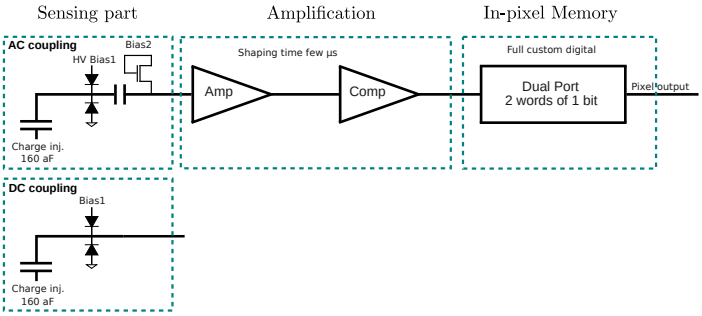

Figure 2. Block diagram of the AC (top) and DC (bottom) coupled pixels.

1.1 Sensor design

The realisation of MIMOSIS relies on an industrial 180 nm CMOS imaging process. The sensor will feature 1024 columns of 504 pixels, the latter being 30 µm × 27 µm wide. Each pixel integrates a complete amplifier/shaper/discriminator chain, inspired by the read-out architecture of the ALPIDE sensor equipping the ALICE-ITS2 detector [4]. If the signal charge related to a particle hit exceeds the discriminator threshold, the analogue front-end samples and holds this information. At the end of a 5 µs long integration time (frame), the hit information is forwarded to an output memory of the pixel. The output memories of the 1008 pixels composing two neighbouring columns are read out by a common priority encoder and sent via two levels of data concentration stages to an elastic buffer. The bandwidth of the buffers and data buses upstream of the elastic buffer are foreseen to treat a burst rate of up to 80 MHz/cm^2 and to buffer this information for consecutive bursts over a duration of up to 50 µs. The output of the elastic buffer sends the data obtained via up to eight data links of 320 Mbps each. This data interface allows for a continuous average data rate corresponding to up to 20 MHz/cm^2 (depending on the distribution of hits and data formatting overhead). This data handling circuitry, incorporating an elastic buffer, reflects the assumption that the intensity of the beam delivered to CBM will fluctuate by roughly a factor of three around its average value. More information on the motivation and the concept of the data buffers can be found in [5].

MIMOSIS-1, shown in figure 1, is a full size prototype containing all features mentioned above but still missing a few components, e.g. concerning single event effect protection and on-chip cluster finding, which will be implemented in the next prototyping step. The sensor was manufactured with wafers composed of a 25 µm thick epitaxial layer. It hosts two arrays of traditional DC-coupled pixels as known from ALPIDE, which are internally denoted as type A and B. They are operated with a back-bias voltage of typically −3 V allowing to deplete (partially) the sensitive volume. The sensor also hosts two AC-coupled pixel flavours (denoted C and D), which allow to top bias the sensor with depletion voltages raising up to 30 V or more. A block diagram of both pixel types is depicted in figure 2.

The pixel array is divided into four sub-arrays reflecting the four pixel flavours. From left to right, the arrangement is as follows: 128 columns with DC-pixels (sub-array A), 384 columns with DC-pixels (sub-array B), 384 columns with AC-pixels (sub-array C) and 128 columns with AC-pixel (sub-array D). Sub-arrays A and B differ by design details of the in-pixel pre-amplifier transistors; similar variations differentiate AC-pixels composing sub-arrays C and D. These design variants are motivated by the search for enhanced radiation tolerance.

2023 JINST 18 C06013

Neither a significant degradation of the pixel performance nor an added value was observed among these pre-amplifier variants. The studies presented here concentrate therefore on sub-arrays B and C.

MIMOSIS-1 was fabricated with different epitaxial layer profiles: a standard (i.e. uniformly doped) layer and a few alternatives with doping profile modifications proposed in [6, 7] to extend the epitaxial layer depletion. A cross-section of the sensing elements denoted as "standard", "p-stop" and "n-gap" is shown in figure 3. These epitaxy variants were produced on separate wafers, each hosting the four pixel types A-D. Thus, a total of 12 combinations of pixel micro-circuits and sensing elements were studied. The standard epitaxy tends to remain partially depleted, which benefits to charge sharing and thus to the spatial resolution. This holds in particular if low depletion voltages are applied, a typical situation encountered with DC-pixels. Instead, the "p-stop" and "n-gap" variants are designed to reach full depletion, in particular if being combined with the high depletion voltages available in AC-pixels. A drawback is a reduced charge sharing, which hampers improving the pixel's spatial resolution by exploiting centre-of-charge arguments. Therefore, depleting the pixels was expected to deteriorate (moderately) the spatial resolution.

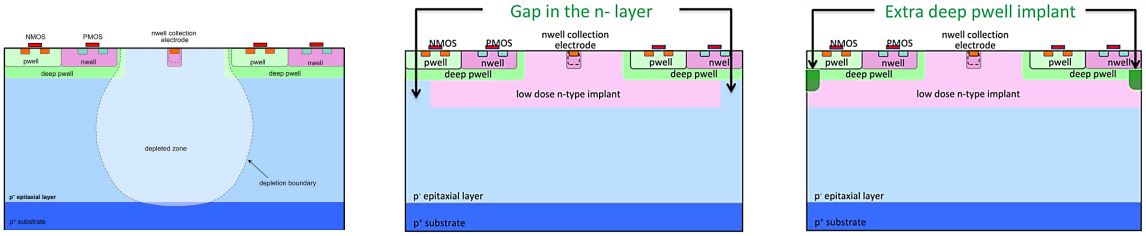

(a) Standard (b) "n-gap" (c) "p-stop"

Figure 3. Three different sensing node, viz. epitaxy doping profile, options used in MIMOSIS-1. Reprinted from [6], Copyright 2017, with permission from Elsevier.

2 Experimental conditions

2.1 Irradiation procedure

Several MIMOSIS-1 chips were irradiated with X-rays at the Karlsruhe Institute of Technology, Germany. The irradiation was performed at room temperature and with a rate of ~280 kRad/h using a 60 kV X-ray generator with tungsten anode and vanadium filter. The dosimetry was carried out by the operators of the X-ray source. Its uncertainty is considered to amount to about 10%. The sensors were operated with nominal slow control settings and voltages during the irradiation. Moreover, a voltage of 10 V was applied to the AC-pixels and the back-bias voltage was set to −3 V. The irradiated sensors were stored at room temperature and tested afterwards.

2.2 Noise measurement

The sensors were tested in the laboratory to study their discriminator threshold dispersion and noise performance. For this purpose, the pixels were pulsed via charge injection upstream of the pre-amplifier and their response was recorded for a wide range of threshold values. For each

2023 JINST 18 C06013

threshold setting, the pulse amplitude was initially set below threshold and raised step by step until all pulsed pixels responded. This "threshold scan" was repeated at least hundred times for each threshold setting. For each step, the fraction of pixels fired was recorded and treated as a probability describing an error-function, the so-called "S-curve". The derivative of the curve obtained for each individual pixel exhibits a Gaussian shape, its width expressing the pixel (thermal) noise while the curve inflection point defines its threshold. The distribution of the threshold values found for each pixel was roughly Gaussian. Its mean value was interpreted as the (average) threshold of the pixel matrix for a given setting. The width of the distribution is a measure of the dispersion of the thresholds of the individual pixels and often referred to as Fixed Pattern Noise (FPN). The FPN is of relevance since the pixels of MIMOSIS-1 are not equipped with individual trim DACs as the latter would be too sizeable. Threshold values are thus viable as long as the number of pixels exhibiting a particularly unfavourable threshold remains small. Due to the long time required for the measurement, only about one third of the pixels, essentially located in the centre of the pixel array, were scanned. The validity of this approach was confirmed by comparing the results with those of scans of the full matrix for selected points.

The pixel threshold values were normalised to units of electron charge relying on the knowledge of the capacitance of the pulse injection capacitor. The design capacity of those capacitors amounts 160 aF (1e/mV). This value is used in the following although it still needs experimental confirmation and being aware that related simulations indicate that shifts as large as ~50 % are not excluded. This uncertainty affects the electron-axis of all plots shown in this work. Efforts to reduce the uncertainty have been initiated, which are expected to end up with a more accurate conversion factor.

2.3 The MIMOSIS-1 beam telescope and data analysis

To measure their detection efficiency and spatial resolution, the sensors were tested with a telescope composed of six planes of MIMOSIS-1 chips. The sensors were wire-bonded to a PCB and individually placed in a temperature stabilised dark chamber operating with a coolant temperature of 15 °C. The planes are 1.5 cm distant. The two outer pairs of sensors were operated as reference planes and equipped with 60 µm thin sensors featuring a standard epitaxial layer for the sake of optimal spatial resolution. The two middle sensors were operated as Devices Under Test (DUT). All sensors were operated in a synchronised way. A scintillator hodoscope was available in case of trigger needs, but it was decided to operate the sensors in free streaming mode during the measurements summarised hereafter.

The data was processed with the TAF data analysis package [8]. Hits from typically 5 consecutive frames were merged during the data analysis to reduce artefacts introduced by the few 100 ns time walk of the pixels [5] in a simple way. A reference track was considered as identified if it was detected by all four reference planes and a particle was considered as detected by the DUT if a hit was found within less than 100 µm from the hit projected from a reference track. The resolution was derived from the distance between the extrapolated beam particle hit position and the closest hit found in the DUT within the search window. The centre-of-gravity of the hit clusters was computed to improve the spatial resolution of all detector planes. We assume a resolution on the extrapolated hit position of 2.5 ± 0.5 µm. Moreover, a multiple scattering term of 1.5 ± 0.15 µm was accounted for. The sensor dark rates were measured in beam test position with activated telescope. A marginal amount of pixels exhibiting an individual dark rate above 10^{-3} were masked offline. This affected

2023 JINST 18 C06013

less than 10^{-4} of the pixels composing the sub-array under test even for the lowest threshold values considered. The results reported in this paper are based on tests performed at DESY with a ~5 GeV electron beam of a few kHz particle rate turning into $\ll 1$ track per frame in average.

3 Results

3.1 Noise and threshold

Typical values of the thermal noise and FPN observed with MIMOSIS-1 are shown in figure 4. The measurement was recorded with the AC-coupled pixels of "p-stop" epitaxial layer; it illustrates the behaviour of the other pixel and epitaxial layer variants. One observes that the thermal noise is ~4.5 e ENC (Equivalent Noise Charge) before irradiation while the FPN varies from 6 to 8 e ENC depending on the threshold value. The thermal noise raises to ~6 e ENC and ~12 e ENC for sensors exposed to integrated doses of 1 and 5 MRad respectively, while the FPN raises and stays between 8 e ENC and 13 e ENC, depending on the threshold value, for both irradiation doses. It is noticeable that the thermal noise remains modest even after the highest dose applied and although the sensor was operated at a stabilised room temperature.

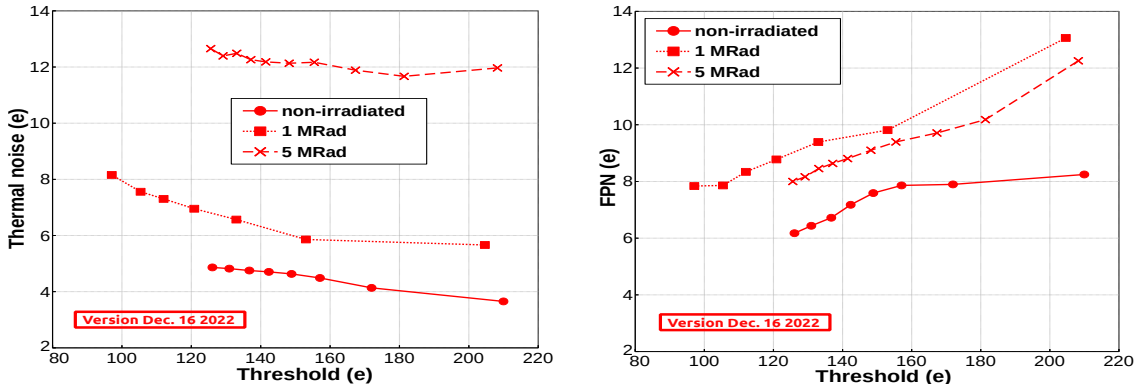

Figure 4. Thermal noise (left) and FPN (right) as a function of the pixel discriminator threshold and of the integrated ionising radiation dose, for the AC-pixel with "p-stop" epitaxial layer, operated with −3 V back-bias and 10 V top-bias voltages.

3.2 Beam tests results

Beam tests of irradiated sensors were performed with chips made of standard and "p-stop" epitaxial layers. A thinned "n-gap" based sensor was also irradiated but was damaged during handling. The "n-gap" measurements were repeated but the data is still under analysis. All results displayed in figures 5, 6, 7 and 8 were obtained with a −3 V back-bias voltage, together with 10 V top-bias in case of the AC-coupled pixels. Figure 5 compares the detection efficiencies observed with irradiated and non-irradiated sensors. They all exhibit an excellent detection efficiency close to 100% for thresholds below 180 e, independently of the radiation dose. For higher threshold values, AC-pixels with standard epitaxial layer exhibit an essentially modest performance decrease. Surprisingly, the decrease is most pronounced for the non-irradiated sensor, while the irradiated sensors show better performances. This may reflect the still preliminary aspect of the studies: for instance, the possibility

2023 JINST 18 C06013

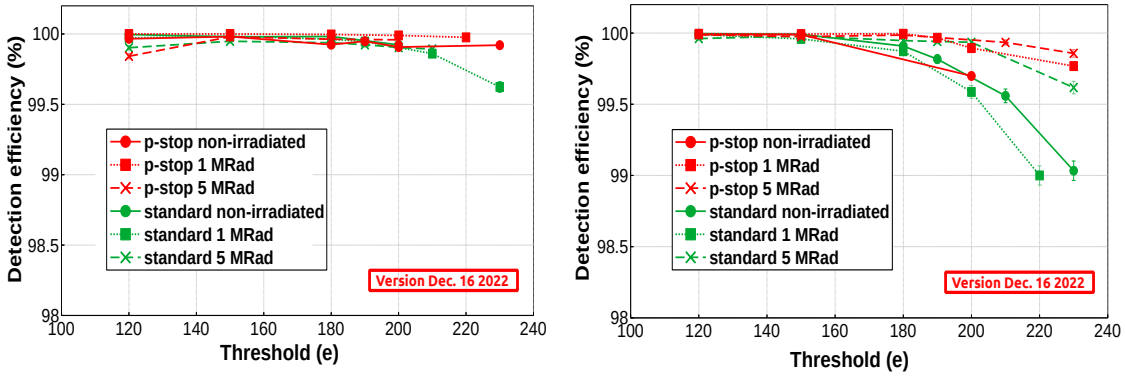

Figure 5. Detection efficiency versus threshold for DC- (left) and AC-pixels (right) in case of standard and "p-stop" epitaxial layers, as a function of radiation dose.

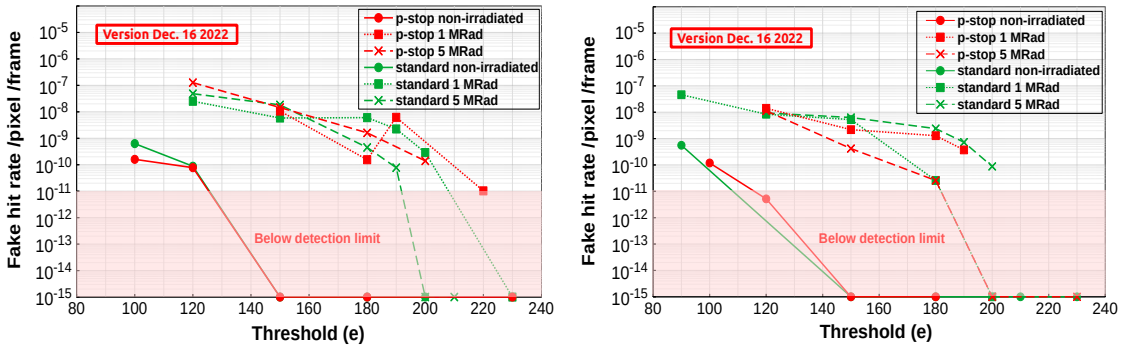

Figure 6. Fake hit rate versus threshold for DC- (left) and AC-pixels (right) in case of standard and "p-stop" epitaxial layers, as a function of radiation dose.

that the steering voltages used during the beam tests were not yet fine-tuned at the same degree for all chips is not excluded and leaves room for improvement. The related dark rates recorded are shown in figure 6. One observes that the dark rate of the non-irradiated pixels remains marginal. After irradiation, it increases by orders of magnitude but remains below the 10^{-6} per pixel readout level, which complies with the MVD requirements. This result was obtained while masking less than 10^{-4} of all pixels under test as discussed previously.

The cluster multiplicities of the sensors and the related spatial resolutions are shown in figure 7 and figure 8, respectively. Higher cluster multiplicities are beneficial for improving the resolution by computing the centre-of-gravity of the clusters. The resolution displayed holds along the short dimension of the non-squared pixel, the resolution found in the other dimension being about 10% worse. As expected, the cluster multiplicity shrinks with enhanced depletion, the DC-pixel with standard epitaxy exhibiting the largest clusters while the AC-pixel with "p-stop" epitaxy offers the smallest ones. This is reflected in the spatial resolution, which varied between about 4 µm and 6 µm, depending on pixel and threshold. We observe that the cluster multiplicity and the resolution are essentially not affected by the radiation dose, which meets our expectation for ionising radiation.

2023 JINST 18 C06013

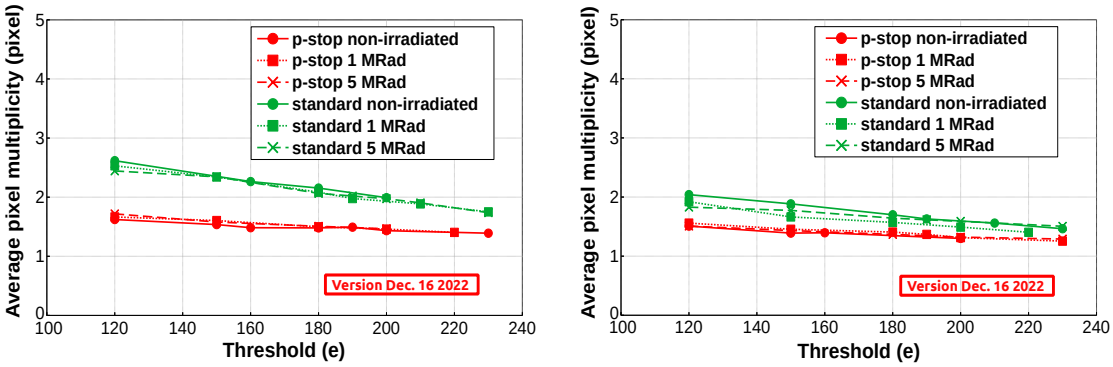

Figure 7. Average pixel multiplicity versus threshold for DC- (left) and AC-pixels (right) in case of standard and "p-stop" epitaxial layers, as a function of radiation dose.

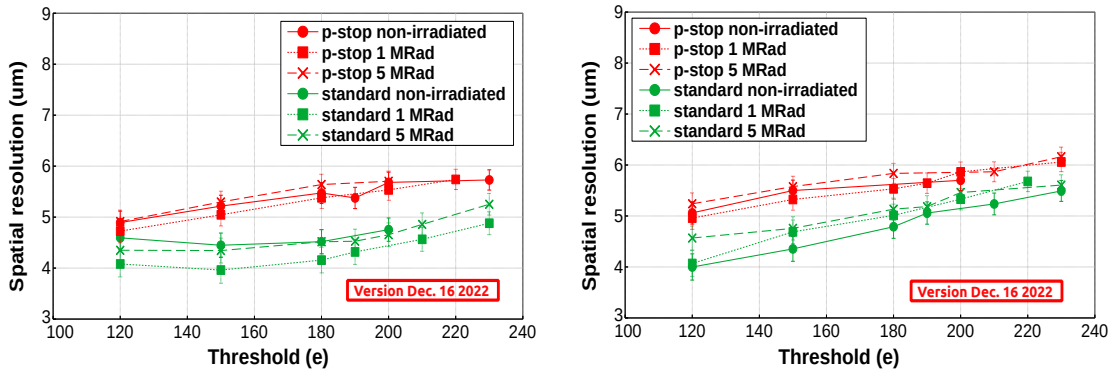

Figure 8. Spatial resolution versus threshold for DC- (left) and AC-pixels (right) in case of standard and "p-stop" epitaxial layers, as a function of radiation dose.

4 Summary and conclusion

MIMOSIS-1, the first full scale prototype of the future MIMOSIS CPS, was tested for its tolerance to ionising radiation. The prototyping investigates among others novel in-pixel circuitry and epitaxial layer variants allowing to enhance the depletion of the sensitive volume.

Several chips were irradiated with ionising doses of up to 5 MRad and tested in the laboratory and with beam particles. After irradiation, one observes a modest increase of the thermal noise and of the FPN. However, both remain at an acceptable level below 14 e ENC for both noise contributions, the highest dose applied and at a stabilised room temperature.

Exposed to beam particles, the irradiated sensors showed a detection efficiency close to 100% for threshold values ranging from about 120 e to 180 e, for all pixels with standard and "p-stop" epitaxial layers. The spatial resolution of the pixels is not significantly influenced by the radiation doses. It is found in the range 4–6 µm, depending on the pixel type and discriminator threshold, as well as on the epitaxy doping profile. No results are yet available on the performance of the "n-gap" pixel, the analysis being still under way. Moreover, the consequences of possible radiation dose gradients crossing the sensor area remain to be studied.

2023 JINST 18 C06013

Overall, the studies realised so far support the statement that MIMOSIS-1 shows excellent performances after being irradiated with integrated doses of up to 5 MRad, thereby satisfying the CBM-MVD requirement.

Acknowledgments

The measurements leading to these results have been performed at the Test Beam Facility of DESY Hamburg (Germany), a member of the Helmholtz Association (HGF). The authors wish to thank the DESY test beam team as much as Alexander Dierlamm and co workers from KIT for their help in irradiating the sensors. This work has been funded and supported by the German federal Ministry of Education and Research (BMBF 05P21RFFC2), the European network for developing new horizons for RIs (Eurizon) and HGS-HIRe for FAIR, HFHF and TANGERINE.

References

[1] J. Stroth et al. eds., *Technical Design Report for the CBM: Micro Vertex Detector (MVD)*, GSI-2022-00549 (2022) [https://fair-center.eu/user/publications/experiment-collaboration-publications#c56056].

[2] CBM collaboration, *Challenges in QCD matter physics –The scientific programme of the Compressed Baryonic Matter experiment at FAIR*, *Eur. Phys. J. A* **53** (2017) 60 [arXiv:1607.01487].

[3] B. Arnoldi-Meadows et al., *Results from single event effect tests with MIMOSIS-1*, 2023 *JINST* **18** C04002.

[4] ALICE collaboration, *ALPIDE, the Monolithic Active Pixel Sensor for the ALICE ITS upgrade*, *Nucl. Instrum. Meth. A* **824** (2016) 434.

[5] M. Deveaux et al., *Observations on MIMOSIS-0, the first dedicated CPS prototype for the CBM MVD*, *Nucl. Instrum. Meth. A* **958** (2020) 162653 [arXiv:1909.05614].

[6] W. Snoeys et al., *A process modification for CMOS monolithic active pixel sensors for enhanced depletion, timing performance and radiation tolerance*, *Nucl. Instrum. Meth. A* **871** (2017) 90.

[7] ATLAS collaboration, *MALTA: a Monolithic Active Pixel Sensor for tracking in ATLAS*, 2020 *JINST* **15** C03019.

[8] IPHC-PICSEL group, *TAF analysis framework*, https://github.com/jeromebaudot/taf.

2023 JINST 18 C06013